

NUMERICAL CALCULATION OF SIMULTANEOUS MASS TRANSFER OF TWO GASES ACCOMPANIED BY COMPLEX REVERSIBLE REACTIONS

R CORNELISSE,† A A C M BEENACKERS,
F P H VAN BECKUM and W P M VAN SWAAIJ

Laboratory for Chemical Reactions Engineering Department of Chemical Engineering, Twente University
of Technology P O Box 217 Enschede The Netherlands

(Received 19 June 1979 accepted 1 October 1979)

Abstract—A discretization technique is described, which makes it possible to calculate numerically mass transfer behaviour between two media in which complex chemical reactions occur. To show the stability of the technique it has been applied to the industrially well-known system of simultaneous absorption or desorption of H_2S and CO_2 to or from an amine solution accompanied by simultaneously occurring strongly interfering overall chemical reaction(s) of complex, non elementary kinetics. For previously published limit cases of the transfer system considered, i.e. for the single transfer of H_2S or CO_2 accompanied by reversible chemical reaction, a comparison has been made with analytical and approximate solutions of previous authors. The agreement is very good. In studying simultaneous transfer of H_2S and CO_2 , on which hardly any previous work was available, special attention has been paid to the effects of the reversibility of the reactions involved. It has been shown how under certain conditions due to reversibility occurring in the transfer zone desorption takes place though absorption would be expected on basis of the driving forces. This revealed that not only enhancement factors larger than unity but also smaller even negative values are possible.

INTRODUCTION

In chemical reaction engineering much work has been done with respect to modelling and calculating the rate of mass transfer in absorption of gases followed by complex chemical reactions [1-10].

Recently the field of desorption from a system involving chemical reactions has also been discussed [11]. However, only a few authors [9, 11] have dealt with simultaneous absorption or desorption of two components accompanied by reversible complex chemical reactions.

A serious problem, when calculating via a mathematical model, the rate of ab- or desorption or in general of mass transfer accompanied by complex chemical reactions, is that the differential equations describing the process, can no longer be solved analytically [10].

Sometimes application of a linearization technique may be advantageous [12, 13] in finding analytical approximate solutions, but this technique may also give erroneous results [14]. A suitable way to acquire results then is to calculate the rate of transfer numerically.

This however is not without numerical problems concerning stability and convergence, particularly in those cases where mass transfer is enhanced by a reaction of more than moderate rate compared to the rate of diffusion of the transferred component near the interface [1, 15].

Although in particular cases these problems can be overcome, the authors felt that in future there would be

a serious need to have available a generally applicable stable technique to calculate mass transfer behaviour disregarding the separation between absorption or desorption of a complex reacting system. This technique must be able to cope not only with systems based on elementary reactions, which has been the issue in almost all previous publications on this subject, but also with systems dealing with complex overall reactions. This technique then supplies the basis from which a computation program can be generated to describe for instance the production in a selectively operated reactor.

Consequently it will be the aim of this contribution to present a discretisation technique for calculating numerically the rate of mass transfer of a complex reacting system.

In order to show the stability of the technique in calculating mass transfer rates it has to be applied to a general type of mass transfer system accompanied by a general type of reaction. A system involving the simultaneous transfer of two components from or to a medium where complex, in principle non elementary, reversible reactions occur with variable rates could have served as a typical example for scrutinizing the convergence behaviour of the discretization technique.

However in the opinion of the authors, without reducing the value of general applicability, it would be preferable to have an issue which is closer to practice, i.e. to apply the technique to a typical but of course more pin-pointed, industrially important reaction system, which implies as much complexity as necessary.

We chose the selective simultaneous transfer of hydrogen sulphide and carbon dioxide into or out of an

†Present address Shell Internationale Petroleum Maatschappij, Treating Division, The Hague, The Netherlands

aqueous solution of a secondary or primary amine [7, 16–18], to serve as illustrative complex reaction system. It is the basic principle of various well-known processes, licensed for (selective) scrubbing of industrial gases.

CHEMISTRY

The kinetics of this system have been reported previously [16, 19–23]. The reaction of H_2S with an amine is reversible and instantaneous compared to mass transfer. This means that, according to reaction (I) at every place in the liquid and at any time equilibrium exists between the participating components related by eqn (1)



The net forward rate of reaction of H_2S is not defined since it represents the difference between the forward and reverse reaction of (I), both of which can be considered infinitely fast [2].

$$K_{H_2S} = [HS^-][R_2NH_2^+]/([H_2S][R_2NH]) \quad (1)$$

$$K_{CO_2} = [R_2NCOO^-][R_2NH_2^+]/([CO_2][R_2NH]^2) \quad (2)$$

The reaction (II) of CO_2 has also to be considered reversible but it is in general not instantaneous with respect to mass transfer. This reaction results in the formation of a carbamate (R_2NCOO^-) and an ammonium ($R_2NH_2^+$) ion. The net forward reaction rate of CO_2 per unit of volume is given [19] by relation (3)

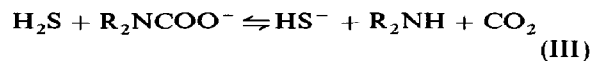
$$R = k_2([CO_2][R_2NH] - \frac{1}{K_{CO_2}} \frac{[R_2NCOO^-][R_2NH_2^+]}{[R_2NH]}) \quad (3)$$

The concentration of the various components in (3) are the actual concentrations in the liquid which need not necessarily be in equilibrium according to relation (2).

Both reactions are non-elementary [16, 19]. Reaction (I) is obtained by combination of the instantaneously occurring dissociation of H_2S and protonation of the amine. Reaction (II) is the result of addition of the same protonation reaction of the amine to the elementary carbamate formation of moderate rate. In both cases it is permissible to represent the reaction system by overall reactions, since the basically occurring and rate-determining elementary reactions are followed by an instantaneous proton transfer.

By dealing with overall reactions the amount of parameters and variables involved can be reduced substantially. In case reaction (I) and (II) occur simultaneously, analogously a further simplification can be obtained by subtraction of the reaction (II)

from reaction (I), thus yielding the overall reaction (III)

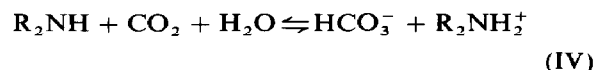


This is allowed, since the overall reaction (I) is also instantaneous. However, we shall still maintain the individual reactions (I) and (II) in basic reaction system. The elimination of the ammonium concentration does not allow of studying the mass transfer behaviour of either reaction (I) or (II), which in our opinion would restrict the scope of this contribution too drastically.

It will be evident that when we study mass transfer behaviour under conditions in which reaction (I) and (II) occur simultaneously, it will not make any difference whether we refer to reactions (I) plus (II) or to reaction (III).

With respect to the latter it may already be disclosed that simultaneous mass transfer may be accompanied by interesting phenomena. By nature of the overall reaction (III) we may imagine that simultaneous absorption or desorption might introduce counteracting effects. The presence of one of the transferred components can locally suppress the transfer of the other one.

The authors are aware of the fact that the bicarbonate formation (reaction (IV)) might also play a role in absorption of CO_2 in an amine solution



The rate of reaction of the latter is so small, however, compared to mass transfer, that this reaction will only contribute to the composition of the bulk. In order to simplify the bulk composition calculations, we shall state that the bulk contains a certain amount of ammonium bicarbonate, realizing that in reality this would be an equilibrium-dependent parameter.

For the sake of convenience the above quoted reactions are denoted for an amine of the R_2NH type, i.e. for a secondary amine which comprises two identical aliphatic side groups. Naturally the reactions will also be valid for other secondary or primary amines. Only sterically hindered secondary amines do not display the carbamate formation (II).

The mass transfer model

We shall describe mass transfer in the gas phase by means of the stagnant film model while for the liquid phase Higbie's penetration model will be used. The reason for using the penetration model for the liquid phase is that for mass transfer with complex chemical reaction the penetration theory is supposed to be more realistic. As no reaction takes place in the gas phase, the simple film theory can be chosen here. The latter also results in a suitable form of the boundary conditions at the interface.

The phenomena of simultaneous diffusion in the gas phase and diffusion plus reversible reaction in the liquid near the interface are denoted as follows

the carbondioxide reaction balance

$$\frac{\partial[\text{CO}_2]}{\partial t} = D_{\text{CO}_2} \frac{\partial^2[\text{CO}_2]}{\partial x^2} - k_2[\text{CO}_2][\text{R}_2\text{NH}] + \frac{k_2}{K_{\text{CO}_2}} \frac{[\text{R}_2\text{NCOO}^-][\text{R}_2\text{NH}_2^+]}{\text{R}_2\text{NH}} \quad (4)$$

the total carbondioxide balance

$$\frac{\partial[\text{CO}_2]}{\partial t} + \frac{\partial[\text{R}_2\text{NCOO}^-]}{\partial t} = D_{\text{CO}_2} \frac{\partial^2[\text{CO}_2]}{\partial x^2} + D_{\text{R}_2\text{NCOO}^-} \frac{\partial^2[\text{R}_2\text{NCOO}^-]}{\partial x^2} \quad (5)$$

the total sulphur balance

$$\frac{\partial[\text{H}_2\text{S}]}{\partial t} + \frac{\partial[\text{HS}^-]}{\partial t} = D_{\text{H}_2\text{S}} \frac{\partial^2[\text{H}_2\text{S}]}{\partial x^2} + D_{\text{HS}^-} \frac{\partial^2[\text{HS}^-]}{\partial x^2} \quad (6)$$

the total amine balance

$$\frac{\partial[\text{R}_2\text{NH}]}{\partial t} + \frac{\partial[\text{R}_2\text{NH}_2^+]}{\partial t} + \frac{\partial[\text{R}_2\text{NCOO}^-]}{\partial t} = D_{\text{R}_2\text{NH}} \frac{\partial^2[\text{R}_2\text{NH}]}{\partial x^2} + D_{\text{R}_2\text{NH}_2^+} \frac{\partial^2[\text{R}_2\text{NH}_2^+]}{\partial x^2} + D_{\text{R}_2\text{NCOO}^-} \frac{\partial^2[\text{R}_2\text{NCOO}^-]}{\partial x^2} \quad (7)$$

the acid balance

$$\frac{\partial[\text{H}_2\text{S}]}{\partial t} + \frac{\partial[\text{CO}_2]}{\partial t} + \frac{\partial[\text{R}_2\text{NH}_2^+]}{\partial t} = D_{\text{H}_2\text{S}} \frac{\partial^2[\text{H}_2\text{S}]}{\partial x^2} + D_{\text{CO}_2} \frac{\partial^2[\text{CO}_2]}{\partial x^2} + D_{\text{R}_2\text{NH}_2^+} \frac{\partial^2[\text{R}_2\text{NH}_2^+]}{\partial x^2} \quad (8)$$

Relation (8) states that the accumulation of acid available in the form of H_2S , CO_2 and R_2NH_2^+ is equal to the net inflow by diffusion of H_2S , CO_2 and R_2NH_2^+

Equilibrium eqn (1) replaces the reaction balance for H_2S

The bulk of the liquid is assumed to be in equilibrium for a given loading of carbondioxide and hydrogensulphide. Accordingly, in terms of the Higbie model, the composition of the package is denoted as

follows

$$\text{for } \begin{cases} t = 0, & x \geq 0 \\ t \neq 0, & x = \infty \end{cases}$$

$$[\text{CO}_2] + [\text{R}_2\text{NCOO}^-] = C_2 \quad (9)$$

$$[\text{H}_2\text{S}] + [\text{HS}^-] = C_1 \quad (10)$$

$$[\text{R}_2\text{NH}] + [\text{R}_2\text{NH}_2^+] + [\text{R}_2\text{NCOO}^-] = Am \quad (11)$$

$$[\text{H}_2\text{S}][\text{R}_2\text{NH}]/([\text{HS}^-][\text{R}_2\text{NH}_2^+]) = 1/K_{\text{H}_2\text{S}} \quad (1)$$

$$[\text{CO}_2][\text{R}_2\text{NH}]^2/([\text{R}_2\text{NCOO}^-][\text{R}_2\text{NH}_2^+]) = 1/K_{\text{CO}_2} \quad (2)$$

$$[\text{R}_2\text{NCOO}^-] + [\text{HS}^-] + [\text{HCO}_3^-] = [\text{R}_2\text{NH}_2^+] \quad (12)$$

Equations (9)–(11) evaluate the initial loadings of the package, while eqns (1) and (2) suppose equilibrium for reaction (I) and (II) at $t = 0$ and at infinite depth. Equation (12) represents the electrical charge balance.

The additional boundary conditions for $x = 0$ and $t \geq 0$ are

$$kg_2 \left([\text{CO}_2]_g - \frac{[\text{CO}_2]}{m_2} \right) = \lambda - D_{\text{CO}_2} \frac{\partial[\text{CO}_2]}{\partial x} - D_{\text{R}_2\text{NCOO}^-} \frac{\partial[\text{R}_2\text{NCOO}^-]}{\partial x} \quad (13)$$

$$kg_1 \left([\text{H}_2\text{S}]_g - \frac{[\text{H}_2\text{S}]}{m_1} \right) = -D_{\text{H}_2\text{S}} \frac{\partial[\text{H}_2\text{S}]}{\partial x} - D_{\text{HS}^-} \frac{\partial[\text{HS}^-]}{\partial x} \quad (14)$$

$$D_{\text{R}_2\text{NH}} \frac{\partial[\text{R}_2\text{NH}]}{\partial x} + D_{\text{R}_2\text{NH}_2^+} \frac{\partial[\text{R}_2\text{NH}_2^+]}{\partial x} + D_{\text{R}_2\text{NCOO}^-} \frac{\partial[\text{R}_2\text{NCOO}^-]}{\partial x} = 0 \quad (15)$$

$$\frac{\partial[\text{R}_2\text{NCOO}^-]}{\partial x} = 0 \quad (16)$$

$$D_{\text{R}_2\text{NH}} \frac{\partial[\text{R}_2\text{NH}]}{\partial x} + D_{\text{HS}^-} \frac{\partial[\text{HS}^-]}{\partial x} = 0 \quad (17)$$

Relation (1) completes the set of these boundary conditions. Relations (13) and (14) equal the transfer rates at the gas and liquid side of CO_2 and H_2S respectively. Equation (15) states that no amine can pass the interface, while eqn (16) expresses that no R_2NCOO^- can pass the interface nor can be converted infinitely fast into CO_2 .

Equation (17) gives the analogue for HS^- , but now HS^- may be converted into H_2S instantaneously, with conversion of R_2NH_2^+ into R_2NH (I). The sum of the diffusion rates at $x = 0$ of HS^- and R_2NH therefore has to be zero.

The enhancement factors ϕ_1 and ϕ_2 of H_2S and CO_2 respectively are defined as

$$2\sqrt{\frac{D_{H_2S}}{\pi\tau}}([H_2S]_{x=0} - [H_2S]_{x=\infty})\phi_1 = \frac{1}{\tau_0} \int_0^{\tau} \left\{ -D_{H_2S} \frac{d[H_2S]}{dx} \Big|_{x=0} - D_{HS^-} \frac{d[HS^-]}{dx} \Big|_{x=0} \right\} dt \quad (18)$$

$$2\sqrt{\frac{D_{CO_2}}{\pi\tau}}([CO_2]_{x=0} - [CO_2]_{x=\infty})\phi_2 = \left\{ \frac{1}{\tau_0} \int_0^{\tau} -D_{CO_2} \frac{d[CO_2]}{dx} \Big|_{x=0} \right\} dt \quad (19)$$

where τ is the contact time of the stagnant element with the gas phase

Numerical treatment

For the sake of convenience in the numerical treatment of the system the equations have been transformed into a dimensionless form (see Appendix)

The numerical method for solving the parabolic differential equations is essentially the three-point backward scheme by Baker and Oliphant [24]

Accordingly the diffusion eqn (20)

$$\frac{\partial U}{\partial \theta} = r \frac{\partial^2 U}{\partial z^2} \quad (20)$$

is discretized as follows. At any $z = z_i = z_0 + ih$, $\theta = \theta_{j+1} = (j + 1)k$ of a rectangular grid (Fig 1) the second derivative of U with respect to z is replaced by (21)

$$\frac{\partial^2 U_i^{j+1}}{\partial z^2} = (U_{i-1}^{j+1} - 2U_i^{j+1} + U_{i+1}^{j+1})/h^2 \quad (21)$$

and for the time derivative of U the three-point backward formula (22) is substituted

$$\frac{\partial U_i^{j+1}}{\partial \theta} = \frac{3U_i^{j+1} - 4U_i^j + U_i^{j-1}}{2k} \quad (22)$$

Here i and j denote respectively the number of (discrete) steps (h) in distance in the observed stagnant volume away from the interface and the number of discrete steps (k) in time, counting from the moment when the liquid volume contacts the gas phase

Thus at every z_i we obtain a linear algebraic equation in which a linear combination of U_{i-1} , U_i and U_{i+1} at time level $j + 1$ is expressed in U value at the previous time levels j and $j - 1$

Denoting the equations subsequently in natural order $i = 0, 1, 2, \dots, m - 1$, a system of linear equations is obtained. This system can be represented in the

vector notation (23)

$$AU = B \quad (23)$$

A being the coefficient matrix, U the unknown vector $U = [U_0^{j+1}, U_1^{j+1}, \dots, U_{m-1}^{j+1}]$ and B the vector built up from the right sides of the difference equations (Fig 2)

Matrix A is tridiagonal. It contains only non-zero entries on the main diagonal and its mutual parallels. The top row and the bottom row of A need further explanation. In the bottom row, corresponding with $z = z_m$, we find that U_m^{j+1} in (21) can be replaced by the known concentration at infinite depth in the liquid, and so it can be moved to the right-side vector B . The top row has a linkage to the conditions at $z = z_0$. A boundary condition at $z = z_0$, given in the form of equation (24)

$$\frac{\partial U}{\partial z} = \alpha U + \beta \quad (24)$$

can be incorporated in the second order Taylor expansion of U at $z = z_0$ (25)

$$U_1^{j+1} = U_0^{j+1} + h \frac{\partial U^{j+1}(z_0)}{\partial z} + \frac{h^2}{2} \frac{\partial^2 U^{j+1}(z_0)}{\partial z^2} + \dots \quad (25)$$

Substitution eqn (20) in (25) and discretising the time derivate with the three-point backward formula (22) we deduce

$$U_1^{j+1} = U_0^{j+1} \left(1 + h\alpha + \frac{3}{4} \frac{h^2}{kr} \right) + \beta h + \frac{h^2}{4kr} (-4U_0^j + U_0^{j-1}) \quad (26)$$

Consequently we see that the first and the bottom row of A involve only two unknowns

Starting from the known situation at $j = 0$ the system may be solved, yielding U at time level $j = 1$ and by repetitive substitution of this solution as starting point for the next $j + 1$ point, the whole scheme moves forward eventually yielding U^n containing the concentrations U_i^n at time $\theta = nk = 1$ in all grid points z_i , $i = 0, \dots, m - 1$

The truncation error of the method is $\mathcal{O}(h^2, k^2)$, stability has been proved in [30]

Extension to the full set of parabolic equations

The basic idea explained in the previous section can be applied to the full problem. At a point $z = z_i$ we now have to discretize five parabolic differential equations instead of one. Thus system $AU = B$ becomes much larger

Every U_i in Fig 2 is replaced by a vector $(p1_i, b_i, a1_i, a2_i, p_i, p2_i)$ representing the (dimensionless) concentrations (see Appendix I) of the six species at

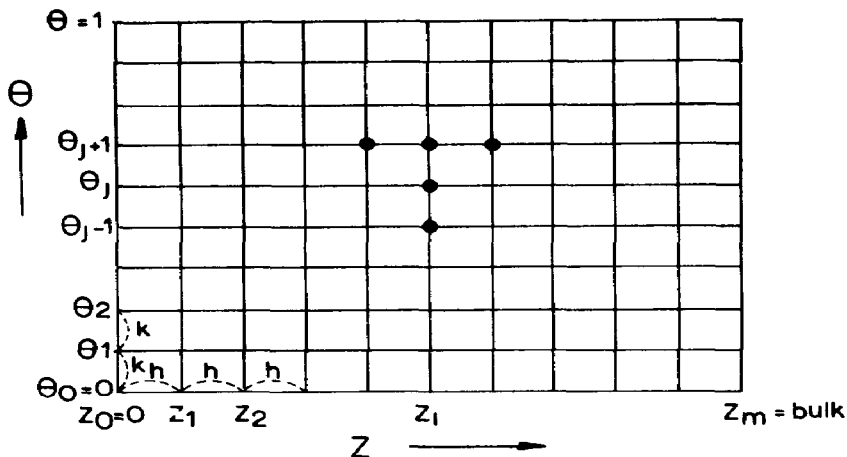


Fig 1 The time/distance space for a discrete evaluation is pictured in the form of a rectangular grid. The cross points represent the discrete values of distance variable z and time variable θ where the concentration vector U_i^j is evaluated. The accented points indicate that the discretization method connects the evaluation of U_i^{j+1} to U_{i+1}^{j+1} , U_{i-1}^{j+1} , U_i^j and U_i^{j-1} .

$z = z_i$ and $\theta = \theta_{j+1}$. In connection with this, every element of matrix A denoted by * in Figure 2 is replaced by a submatrix having six columns and five rows. The sixth row, which is necessary to make the whole system solvable, is supplied by the equilibrium equation (A6). Finally we have to take into account the production terms in (A3).

Both the equilibrium equation (A6) and the production terms are non linear. They are linearized by the Newton-Raphson method [25].

Accordingly eqn (A6) is replaced by

$$-K_1 \tilde{p} p_1 + \tilde{a} 1 b + \tilde{b} a 1 - K_1 \tilde{p} 1 p = \tilde{b} \tilde{a} 1 - K_1 \tilde{p} \tilde{p} 1 \quad (27)$$

where \tilde{p} , $\tilde{a} 1$, \tilde{b} and $\tilde{p} 1$ are guessed values. A similar linearization is carried out for the production terms of (A3).

If we take $\tilde{a} 1$, $\tilde{b} 1$ etc equal to the value of the corresponding concentrations at the known time level θ_j , the truncation error of this linearization is $O(k^2)$, which is acceptable in view of the last sentence of the previous section.

With m intervals in z direction the matrix A has order $6m$, and now possesses a band of 23 diagonals. Outside these diagonals all entries are zero. The specific sequence p_1, b, a_1, a_2, p, p_2 is found, reducing the number of diagonals from 23 to its lowest possible value of 17. For solving band matrices special subroutines can be written.

FURTHER REFINEMENTS

Iteration

Although the truncation error in the linearized production term is of the same order in k as the discretization error of the differential equation, we did

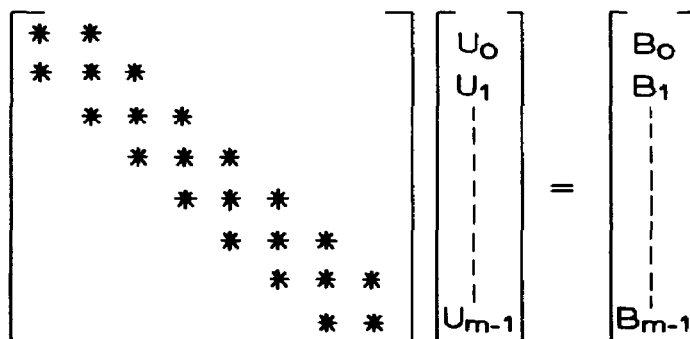


Fig 2 The discretization of the partial differential equations results in a set of linear algebraic equations, which can be represented in a vector notation $AU = B$. The shape of these vectors is depicted above. Eventually upon extension to the full set of five partial differential equations (A1)-(A5) and one equilibrium eqn (A6) it results that every element of the vectors U and B is replaced by a new vector containing the concentration of the six reaction species and accordingly every element of A is replaced by a 6×6 submatrix.

not consider the solution vector U calculated from (23) as the final solution at $\theta = \theta_{j+\frac{1}{2}}$, but only as an improved estimate of the values $\bar{p}1, \bar{b}$ etc, with which the matrix A and the vector B are built up again. Thus a new solution U of system $AU = B$ is obtained and so on until the difference between two successive vectors U is less than a given tolerance. This iteration is of the Newton-Raphson type and exhibits quadratic convergence. For a given tolerance in U of 10^{-6} the last solution of U is accurate to 12 digits. Of course the accuracy still remains subject to the Baker and Oliphant truncation error $\mathcal{O}(h^2, k^2)$.

Transformation of z and θ

Calculations have not been done with constant steps h and k as may have been suggested in the previous sections, but with constant steps in new space and time variables ξ and ω so chosen, that the grid points of the z, θ plane (Fig 1) concentrate near $z = z_0$ where the steepest gradients of $p1, b$ etc occur and at small θ where the gradients of $a1$ and $a2$ can be expected to be maximum.

Most of the computations are based on a grid with 50 points in space and 60 points in time. A typical example is the following. We calculated the area $0 \leq z \leq 8, 0 \leq \theta \leq 1$. Here $z = 8$ corresponds to 8 times the thickness of the film in terms of the film theory. The value of eight was determined empirically in such a way that doubling of this value would introduce a deviation in the enhancement factors of less than one tenth of a percent.

Equally spacing of z and θ would give $h = 0.16$ and $k = 0.0167$. After transformation we have the smallest space interval 0.003 and the smallest time interval 0.0003, which gives a considerably more accurate description of the details of the concentration profiles. Any two transformation functions $\xi(z)$ and $\omega(\theta)$, giving a grid point distribution of desired nature, may be chosen if only the derivative of $\xi(x)$ remains bounded in order to prevent infinite coefficients for the spatial derivatives in the differential equations and the interface conditions.

Finally, ϕ_1 and ϕ_2 are calculated by integration by Simpson's rule using eqns (18) and (19) respectively, in which the derivatives are replaced by combination with eqns (14) and (13) plus (16) respectively.

In the following we shall show the results of calculations on mass transfer behaviour of this reaction system, using the above discretization technique. The results will be compared with previously published analytical and approximate solutions. The comparison will show the applicability of the approximate models. As evidence for the stability of this discretization technique it will further be shown that variation of the dimensionless reaction parameter M or equilibrium constants over more than eight decades will cause no problem concerning stability or convergence in the numerical system. This result has not been published before.

The scope of the contribution, however, will be much wider. For the first time, as far as the authors know, it will be shown how simultaneous transfer of two species is influenced by the reversibility of the reactions involved in the reaction zone, in such a way that desorption of one of the species occurs, though the driving force would predict absorption. This phenomenon of forced enhanced desorption implies that, in addition to the values of the enhancement factors larger than unity, smaller and even negative values can also occur.

The possibility of negative enhancement factors has not been demonstrated before.

RESULTS

In the previous section the phenomenon of simultaneous transfer of two gases in a liquid with counteracting reversible parallel reactions has been described and discretized to be treated numerically.

However nothing has been assumed about the range of values of the various parameters included in the system, such as kg_1, kg_2, m_1, m_2 , the diffusion coefficients, the contact time τ , initial concentrations, equilibrium constants etc. Still, the assumption of these values will be the key in showing the results of the system with regard to the numerical stability and with respect to typical sorption behaviour. Depending on the values of the various parameters the system describes for instance the sorption/reaction schemes as outlined in Table 1.

It would be far beyond the scope of this contribution to give a complete exhibition of the influences of all the various parameters on the enhancement factors ϕ_1 and ϕ_2 .

However it is of interest to demonstrate some of the effects of reversibility on the rate of mass transfer under both absorption and desorption conditions, parallel to the confirmation of the excellent numerical properties.

To restrict the number of variables the larger part of the parameters mentioned above will not be varied and, unless specified elsewhere, they are evaluated to practical values as given in Table 2.

The value of τ is chosen arbitrarily, in the light of the fact that the solution of the system also provides sixty solutions at shorter time levels. These solutions will not be shown. The diffusivities are all taken equal, allowing of a good comparison with the results of previous contributions based on different transfer models. To ensure total liquid-phase resistance to mass transfer the mass transfer coefficients of CO_2 and H_2S in the gas phase are stated to be 100 m/s. However, in those cases where only one of the gas phase components is desired to be transferred the kg of the not-transferred component will be taken as zero.

The concept now is that enhancement factors ϕ_1 and ϕ_2 are a function of $M, K_{\text{H}_2\text{S}}, K_{\text{CO}_2}, \alpha_1$ and α_2 .

The latter two symbols stand for the molar sulphur and carbon-dioxide load per mole amine.

Some particular results will be shown for the following cases of Table 1 (a) scheme 5, which also

Table 1 The Studied simultaneous transfer of H₂S(A1) and CO₂(A2) accompanied by reaction with an amine R₂NH (B) which yields conversion of HS⁻ (P1) R₂NH₂⁺ (P) and R₂NCOO⁻ (P2) comprises several mass transfer regimes as indicated in the table below The various regimes can be generated by appropriate evaluation of the parameters involved The values used in this contribution are indicated The values given between brackets are arbitrarily set

scheme	overall reaction involved	K ₁	K ₂	M	α ₁	α ₂	kg ₁	kg ₂	mass transfer regime
1	A1(g) ⇌ A1(l)	0	(10 ⁻⁴)	(10 ⁻²)	1/>1	(8 06)	0	(0)	physical ab/de-sorption of A1
2	A2(g) ⇌ A2(l)	(10 ⁶)	0	(0 01)	(0)	<1/>1	(0)	0	physical ab/de-sorption of A2
3	A1 + B →	∞	(10 ⁻⁴)	(10 ⁻²)	0	(8 06)	>0	(0)	absorption of A1 followed by instantaneous chemical reactions
4	A2 + 2B →	(10 ⁶)	∞	>0	(0)	1	(0)	0	absorption of A2 followed by irreversible 1 1 order reaction of variable rate
5	A1 + B ⇌ P1+P	>0	(10 ⁻⁴)	(10 ⁻²)	<1/ 1	(8 06)	0	(0)	ab/de-sorption of A1 accompanied by instantaneous reversible reaction
6	A2 + 2B ⇌ P2+P	(10 ⁶)	>0	0	(0)	1 1	(0)	0	ab/de-sorption of A2 accompanied by reversible reaction of variable rate
7	A1 + P2 ⇌ A2 + P1 + B	0	0	0	0	0	0	0	simultaneous sorption of A1 and A2 accompanied by a reversible chemical reaction with complex kinetics
8	A1 + P2 ⇌ A2 + P1 + B	>0	>0	0	0	0	0	0	sorption of A1 accompanied by a reversible overall reaction with complex kinetics (A2 not volatile)
9	A2 + P1 + B ⇌ A1 + P2	>0	>0	0	0	0	0	0	sorption of A2 accompanied by a reversible reaction with complex kinetics (A1 not volatile)

covers in continuity the limit schemes 1 and 3, (b) scheme 6, which also covers in continuity the limit schemes 2 and 4, (c) scheme 7

(a) Sorption of a single component (H₂S) followed by instantaneous reversible reaction at various liquid loadings (α₁) A1 + B ⇌ P + P1

By putting kg₂ = 0, M = 10⁻², K_{CO₂} = 10⁻⁴ and α₂ = 10⁻², the model reduces to mass transfer of one component (H₂S) with instantaneous reaction only (Table 4, Scheme 5) Enhancement factor φ₁ is a

function of K_{H₂S} and α₁ (Fig 3) only Figure 3 shows φ₁ as function of K_{H₂S} at various values of α₁

Every solid line represents a curve for constant α₁ For very small values of K_{H₂S} the reaction between H₂S and free amine does not occur Sulphur is available only in the form of H₂S The liquid acts as physical solvent (Table 1, Scheme 1) φ₁ equals unity for all α₁ both for both absorption and desorption

For infinite values of K_{H₂S} the system reflects absorption followed by instantaneous irreversible reaction (Scheme 3) The enhancement factor,

Table 2 List of parameters entailed in the system, which are prefixed These parameters are evaluated to practical values as indicated above

parameter	value	dimension
τ	8 7 * 10 ⁻⁴	s
Am	2 0	kmole/m ³
m ₁	1 805	-/-
m ₂	0 595	-/-
[H ₂ S] _g	4 17	kmole/m ³
[CO ₂] _g	4 17	kmole/m ³
D _{CO₂}	5 13 * 10 ⁻¹⁰	m ² /s
r ₁	1	-/-
kg ₁	100	m/s
kg ₂	100	m/s
p3	0 02	-/-

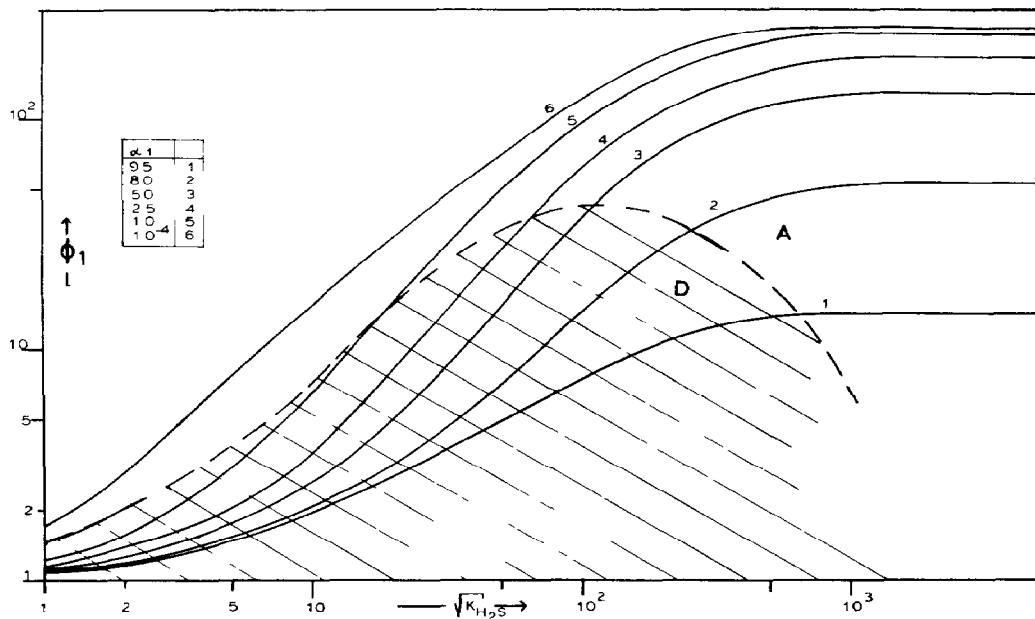


Fig 3 Plot of the enhancement factor of H_2S (ϕ_1) as a function of the equilibrium value $K_{\text{H}_2\text{S}}$ for various sulphur loadings α_1 of the solvent. The plot holds for the conditions as specified in Table 1 (for Schemes 1, 3 and 5) and Table 2 depending on the value of $K_{\text{H}_2\text{S}}$ under these conditions absorption or desorption (dashed area) can occur. The dashed line represents the conditions where no net mass transfer occurs since the gas and liquid phase are in equilibrium ($\alpha_1 = 1$).

calculated numerically, almost exactly meets the theoretically calculated value for this regime

$$\phi_1 = 1 + \frac{[\text{R}_2\text{NH}]}{m_1 [\text{H}_2\text{S}]_g} \quad (28)$$

where $[\text{R}_2\text{NH}]$ stands for the free amine concentration

For intermediate values of $K_{\text{H}_2\text{S}}$, analytical solutions are also available. Secor and Beuttler [26] and recently also Onda *et al* [5] gave a general analytical solution. Olander [2] and Ramachandran [9] presented more particular solutions, which can be derived from the former two. The difference between the numerical solution (Fig 3) and that obtained via Onda *et al* [5] is less than 1%.

In Fig 3 two regimes are shown. The dashed area represents that of desorption ($\alpha_{1\infty} > 1$) and the region above that of absorption ($\alpha_{1\infty} < 1$). A dynamic equilibrium of no net mass transfer occurs for $\alpha_1 = 1$. The line for $\alpha_{1\infty} = 1$ shows a maximum at an intermediate value of $K_{\text{H}_2\text{S}}$. In conformity with this line (though not shown) lines of $\alpha_{1\infty} = \text{constant}$ can also be generated. They likewise display a maximum. This means that at the same driving force liquid phase controlled desorption of H_2S goes faster for a relatively weak base like diisopropanolamine than for a strong base like monoethanolamine. The occurrence of the maximum can be well understood, taking into account the free amine concentration in the bulk, which results from a specified equilibrium constant and the driving

force ($\alpha_{1\infty} - 1$). We conclude that the numerical solution is in good agreement with the analytical solution and that the solutions of Secor and Beuttler [26], Onda *et al* [5], Ramachandran [9] and Olander [2] hold for both absorption and desorption.

(b) Absorption or desorption accompanied by reversible reaction of finite rate ($\text{A}_2 + 2\text{B} \rightleftharpoons \text{P} + \text{P}_2$)

Analogous to the former case, putting $kg_1 = 0$, $K_{\text{H}_2\text{S}} = 10^{+6}$ and $\alpha_1 = 0.01$ results in the transfer of CO_2 without interference of H_2S (Table 1, Scheme 6). Since the reaction of CO_2 is of finite rate, the dimensionless rate constant M is a parameter too, together with K_{CO_2} and α_2 .

To reduce the amount of parameters α_2 has not been varied and is stated to be equal to 0.01. Figure 4 shows the enhancement factor ϕ_2 as a function of \sqrt{M} at various values of K_{CO_2} . For $K_{\text{CO}_2} \ll 10^{-5}$ no substantial conversion of CO_2 can occur in the liquid owing to equilibrium constraints, and, independently of the value of M , unenhanced mass transfer always occurs (ϕ_2 equals unity (Table 1, Scheme 2)). For very large values of K_{CO_2} , ϕ_2 reaches its limit value for instantaneous reaction, the area where kinetics of the reverse reaction and equilibrium constraints do not play a role (Table 1, Scheme 4). Many authors have published for the case of infinite values of K_{CO_2} [5, 12, 13, 27–29]. Some of them gave identical solutions [5, 12, 13]. Wellek *et al* [28] recently gave a comparison of the solutions presented by the various authors. We have restricted ourselves to comparing our results with

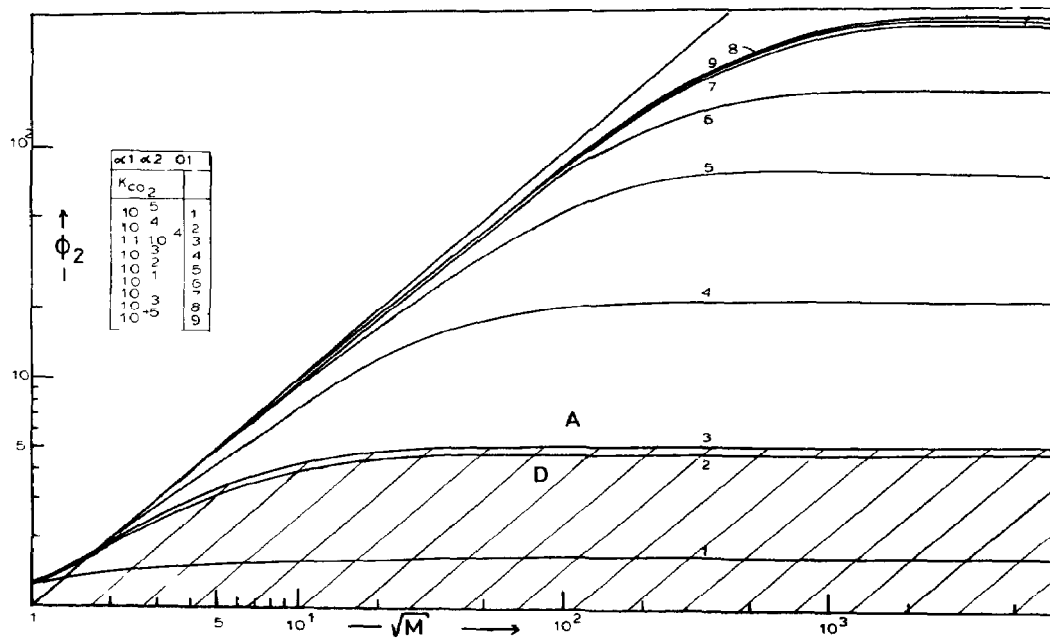
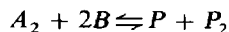


Fig 4 Plot of the enhancement factor of CO_2 (ϕ_2) as a function of the dimensionless reaction rate constant (M) for various values of the equilibrium constant (K_{CO_2}). The plot holds for the conditions as specified in Table 1 (for Scheme 2, 4 and 6) and Table 2. Depending on the value of K_{CO_2} , absorption or desorption (dashed area) can occur. No net mass transfer occurs when gas and liquid phases are in equilibrium ($K_{CO_2} \approx 1.4 \times 10^{-4}$).

those of Hikita [12] and DeCoursey [27]. The difference amounts to less than 3% for both.

Another well-known area indicated in Fig 4 is that where M becomes infinite, i.e. where ϕ_2 reaches its limit value for instantaneous reversible reaction for the reaction type



(analogous to Scheme 3 of Table 1 but for different stoichiometry). Here too several authors [5, 9, 26, 30] have published previously. Secor and Beuttler [26], Onda *et al* [5], presented a solution from which the particular solutions of Danckwerts [30] and Ramachandran [9] can also be derived. The difference between the present numerical solution and that of Onda [5] is less than 1% (see Table 3).

For varying M and K no analytical (approximate) solutions are available. The CO_2 type kinetics are of a non elementary type. No publications are available on this subject. An approximate solution was derived based on that of Onda [5], his eqn (17) being modified to make it applicable to the more complex kinetics discussed in this paper (see eqn 29).

$$M = M \left(\frac{b_i}{q_B} \right) \left(1 + \frac{m+1}{q+1} \frac{v_E T}{r_E} \right) \quad (29)$$

(nomenclature according to Onda)

In spite of this rather crude linearization the agreement found for the circumstances as applied in this contribution, was remarkable. The maximum deviation was 7%.

In Fig 4 two areas have been indicated too. The dashed area represents the area where desorption occurs, the area above that of absorption. Under the

Table 3 Comparison of numerically and analytically [6] calculated values of ϕ_2 for instantaneous reversible reaction of type $A_2 + 2B \rightleftharpoons P + P_2$ as a function of the equilibrium constant K_{CO_2} . Table 7 Schemes 2, 4, 6. For conditions applied, reference is made to Fig 4.

K_{CO_2}	ϕ_2 , num	ϕ_2 , anal
10^5	385.1	383.5
10^3	381.3	379.9
10^1	348.4	347.1
10^{-1}	182.5	182.5
10^{-2}	79.7	79.4
10^{-3}	23.30	23.16
2.98×10^{-4}	10.35	10.28
1.69×10^{-4}	7.17	7.12
1.44×10^{-4}	6.43	6.39
1.11×10^{-4}	5.39	5.36
10^{-4}	5.02	5.00
10^{-5}	1.69	1.69

prevailing conditions the system is approximately in dynamic equilibrium for $K_{\text{CO}_2} = 1.4 \cdot 10^{-4}$. For this K_{CO_2} no net transfer of CO_2 occurs but enhancement factor ϕ_2 still increases with M . The "dynamicity", i.e. the rate of equalizing a small disturbance from the equilibrium between the concentration of CO_2 in the gas and liquid phase, depends on the value of M and is materialized in the value of ϕ_2 . Here again we conclude that the solutions of Onda *et al* [17], Danckwerts [30], Ramachandran [9] and Secor *et al* [26] can be applied to both absorption and desorption.

(c) *Simultaneous absorption of two gases in a reactive liquid, one gas (H_2S) reacting instantaneously, the other with variable rate. Both reactions are in principle of reversible nature* (Table 1, Scheme 7) $A_1 + P_2 \rightleftharpoons P_1 + B + A_2$

In the chemistry section we have already pointed out that at simultaneous mass transfer the two overall reactions I and II can be combined into overall reaction III

The occurrence of this overall reaction III implies that in the presence of a driving force for both H_2S and CO_2 the gas and liquid phase will "try" to reach equilibrium by mass transfer of components which show up at different sides of the reaction equation III. By this characteristic counteracting effects can be expected if both CO_2 and H_2S display the same sign for the driving force and cooperative effects when the signs of the driving forces are different. Another aspect which emerges from reaction III is that it will be impossible to generate a condition which allows both H_2S and CO_2 to react irreversibly if the reaction rate of this overall reaction is instantaneous to mass transfer. At instantaneous reaction equilibrium III will be established not only in the bulk of the liquid but also in the transfer zone near the interface. Consequently in the transfer zone too only one condition can be fulfilled at once. The equilibrium according to reaction III can lie either entirely to the right or to the left. This means that either H_2S or CO_2 can be absorbed without back pressure limitation, i.e. reversibility effects near the interface.

It can even be imagined that, when H_2S absorption is followed by reaction III which lies entirely to the right, the induced CO_2 production (back pressure) in the transfer zone might be so huge that the CO_2 concentration in the transfer zone will locally overshoot the value which is in equilibrium with the concentration in the gas phase. In this case CO_2 will desorb, though the driving force between gas and liquid phase would predict absorption.

For moderate reaction rates, the equilibrium III might not be reached in the transfer zone, especially when the driving forces are large. This will result in a "pseudo" irreversibility for both reactions with respect to mass transfer. The reaction rate in this case is not sufficiently fast compared to the transfer rate of the

gases, that a back pressure can be built up which has a substantial impact on the transfer rate.

In the following we shall show this phenomenon of pseudo irreversibility for the transfer of CO_2 at moderate reaction rates in the event of the transfer of H_2S generating various degrees of depletion via its equilibrium constant ($K_{\text{H}_2\text{S}}$). In addition we shall show the occurrence of reversibility in the transfer zone for a virtually infinite reaction rate.

Figure 5 demonstrates enhancement factor ϕ_2 at moderate values of M for various values of $K_{\text{H}_2\text{S}}$. It shows the effects on the transfer rate of CO_2 for $K_{\text{CO}_2} = 10^5$ for various degrees of depletion of the amine near the interface. The degree of depletion for these cases is dictated by the value of $K_{\text{H}_2\text{S}}$. For $K_{\text{H}_2\text{S}} < 10^{-2}$ no H_2S can be converted into HS^- and the amine concentration is not depleted.

The ϕ_2 curve reflects the enhancement factor for pseudo first order irreversible reaction (see also Table 1, Scheme 3, as discussed above).

Increasing $K_{\text{H}_2\text{S}}$, however, decreases the slope of the ϕ_2 curve. The dictated depletion causes the effective amine concentration as "experienced" by CO_2 to be lower than for the pseudo first order irreversible regime.

Finally, for infinite values of $K_{\text{H}_2\text{S}}$ ($K_{\text{H}_2\text{S}} > 3.1 \cdot 10^5$) complete depletion of the amine is induced. The slope of ϕ_2 does not decrease further with increasing $K_{\text{H}_2\text{S}}$.

For this regime of CO_2 absorption with complete depletion of amine approximate analytical solutions are also available. Goettler and Pigford [7], Ouwkerk [7] and Cornelisse *et al* [14] presented an approximate solution for simultaneous mass transfer of H_2S and CO_2 under irreversible conditions at instantaneous reaction of H_2S .

Up to $M = 10^3$ the difference between the present numerical solution and the approximate solution is less than 3%. This shows that the assumption of pseudo irreversible conditions is valid for the conditions as applied in this contribution. For $M > 10^3$, however, deviations increase drastically. This is due to the influence of reversibility in the transfer zone of reaction III, which the numerical solution takes into account, whereas the approximate analytical solutions do not. The simultaneous absorption of H_2S induces conditions in the transfer zone which force the CO_2 absorption to occur under reversible conditions. The reversibility is forced since under single transfer of CO_2 under the same conditions as studied here no reversibility effects would have been experienced (see Fig. 4).

To show this phenomenon of forced reversibility of CO_2 in a more pronounced manner Figs. 6 and 7 are given. For $K_{\text{CO}_2} = 6.8$ —a value which may occur in practice—Fig. 6 shows that CO_2 absorbs virtually unenhanced for $M = 10^{-2}$. For $M = 10^4$ however the picture becomes entirely different. Though for $M = 10^4$ and $K_{\text{CO}_2} = 6.8$ Fig. 4 would expect ϕ_2 to have a value of about 70—which means that, in the absence of transfer of H_2S , CO_2 absorption would be

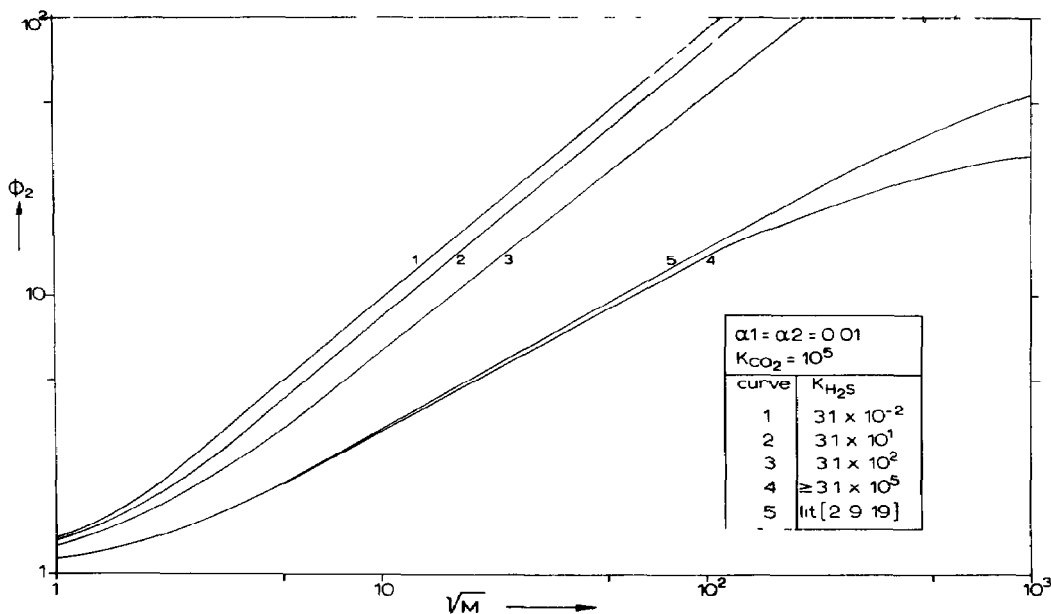


Fig 5 Plot of the enhancement factor ϕ_2 as a function of the dimensionless reaction rate parameter (M) for various degrees of depletion of amine near the interface Table 1, Scheme 7 The depletion is induced by the simultaneous absorption of H_2S The degree of depletion depends on the value of the equilibrium constant of H_2S (K_{H_2S}) The numerical solution 4, deviates from the solutions of previous workers [1, 7, 14] owing to take into account reversibility effects in the transfer zone which previous literature does not take into account The plot holds for conditions as outlined in Table 2

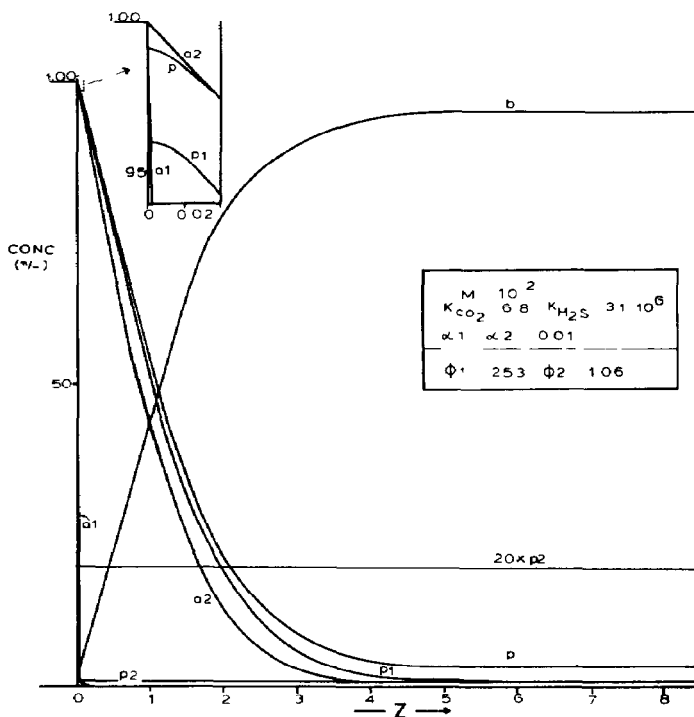


Fig 6 Dimensionless concentration profile at $\theta = 1$ for simultaneous absorption of H_2S (a_1) and CO_2 (a_2) accompanied by instantaneous reaction with the amine (b) for H_2S and slow reaction of for CO_2 The simultaneous case is in behaviour virtually identical with the sum of single H_2S and CO_2 transfer without interference by reaction The conditions applied are those denoted in Table 2 and in the plot itself

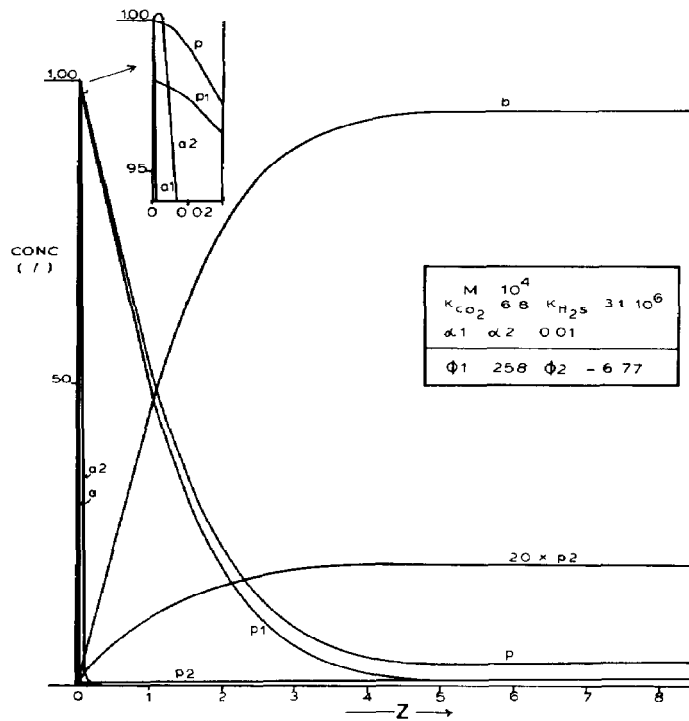


Fig 7 Numerically calculated dimensionless concentration profile at $\theta = 1$ for simultaneous transfer of H₂S (a1) and CO₂ (a2) accompanied by instantaneous reaction with the amine (b) of H₂S and fast reaction for CO₂, Table 1, Scheme 7. Though the driving forces, $(1 - a1_\infty)$ and $(1 - a2_\infty)$, would predict both gases would absorb as in Fig 6, interfacial reversibility induced by the conversion of H₂S causes CO₂ to desorb. This phenomenon of forced desorption materializes in the occurrence of a negative enhancement factor. The conditions applied are the same as for Fig 6.

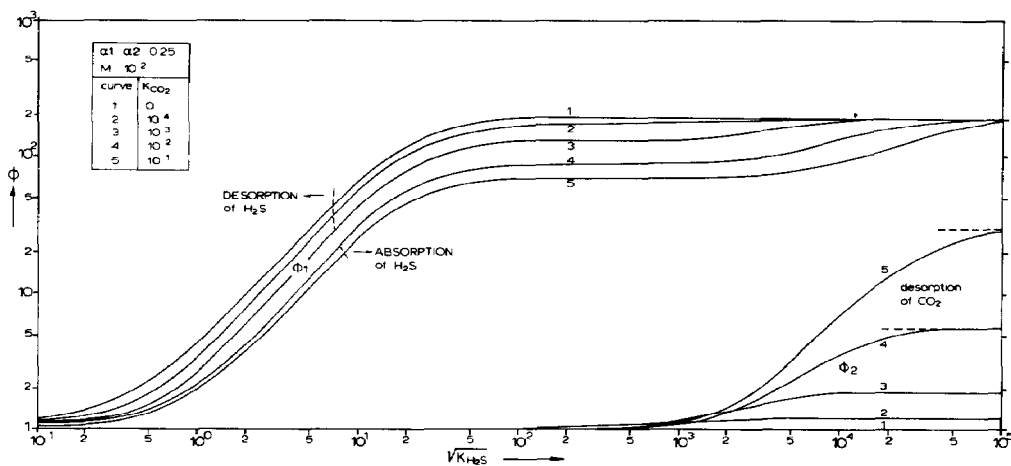


Fig 8 Plot of the enhancement factors of H₂S (ϕ_1) and CO₂ (ϕ_2) as a function of the equilibrium constant of H₂S (K_{H_2S}) for simultaneous transfer of H₂S and CO₂ accompanied by chemical reaction. Table 1. Scheme 7. CO₂ desorbs while H₂S switches (dashed line) from desorption to absorption with increasing K_{H_2S} . The figure shows that though the reaction rate of CO₂ is slow at irreversible H₂S absorption CO₂ will desorb "overenhanced" or even infinitely "overenhanced" by cooperative and forced conversion of the carbamate near the interface. The sensitivity to overenhancement is dependent on the value of K_{CO_2} . The conditions applied are those indicated in Table 2 (excl $p_3 = 0$) and the above figure.

chemically enhanced by a factor of 70—to the contrary Fig 7 reveals that in the presence of H₂S sorption/reaction CO₂ will desorb enhanced by a factor of 6.77. During the contact time θ a back pressure of CO₂ is induced near the interface that overshoots the CO₂ pressure in the gas phase and net desorption follows. Owing to the positive driving force for CO₂ absorption at $\theta = 0$, and an average net desorption of CO₂ for $\theta = 1$, a negative enhancement factor is obtained. This desorption under the circumstances of having a positive driving force $(1 - a2_\infty)$ for absorption will be defined as forced desorption. A consequence of the possible occurrence of forced desorption due to simultaneous absorption of another reactive species is that for such systems the sign of the driving force is no exclusive indication of the direction in which mass transfer will go.

Supplementary to counteracting effects at simultaneous mass transfer cooperative effects may also occur.

Figure 8 shows the dependence of one particular curve of Figure 1, i.e. for $\alpha_1 = 0.25$ on the value of K_{CO_2} under the following conditions: $\alpha_2 = 0.25$, $M = 0.01$ and $p_3 = 0$.

The corresponding desorption curves for ϕ_2 have also been drawn. Since M equals 0.01, hardly any effects of the CO₂ kinetics can be expected. Indeed ϕ_2 equals unity and up to $K_{H_2S} = 90,000$ ϕ_1 can be calculated from Onda's solution [17], similar to the single mass transfer of H₂S described above (Table 1, Scheme 3). For this case, K_{CO_2} influences ϕ_1 only via the bulk composition.

However for $K_{H_2S} > 90,000$ again reversibility effects in the mass transfer zone show up. The amine depletion conditions near the interface, dictated by the degree of irreversibility of the H₂S reaction (I), cause the desorption of CO₂ to be unexpectedly enhanced, or even infinitely enhanced, although its dimensionless reaction rate constant has a small value. Infinitely enhanced desorption of CO₂ occurs for extremely large values of K_{H_2S} . This can be defined as infinitely over enhanced desorption. The numerically calculated limiting value of ϕ_2 is equal to the theoretically expected value for the case when CO₂ desorption is controlled by the supply of p_2 from the bulk to the interface.

$$\phi_2 = 1 + \frac{p2_\infty Am}{(a2_\infty - 1)m_2 [CO_2]_g} \quad (30)$$

In agreement with this we calculate the limit value ϕ_1 as also equal to the theoretical value

$$\phi_1 = 1 + \frac{(b_\infty + 2p2_\infty)Am}{m_1 [H_2S]_g} = 200.3 \quad (31)$$

Since the values of $p2_\infty$ and $a2_\infty$ are a function of K_{CO_2} , we obtain different limit values of ϕ_2 for every K_{CO_2} .

The limit value of ϕ_1 , however, does not vary with K_{CO_2} since for the present conditions and infinite values of K_{H_2S} , the sum of b_∞ and $2p2_\infty$ is equal to $(1 - \alpha_1)$.

The latter value is also the limit value for the case where H₂S absorbs irreversibly and K_{CO_2} equals zero.

Analogous to Fig 8 we could show additional curves for $M = 10, 100$ etc. We think, however, that generating more curves will not contribute any further to showing the excellent behaviour of the discretized system, nor would it illustrate the validity of other approximate models more exclusively. Moreover these curves are so complex, by showing asymptotes for cases where one gas component is in equilibrium with the liquid bulk, while the other gaseous component still causes mass transfer for both gases, that this would need excessive explanation. We therefore finalize this contribution by showing only Figs 9–11 to illustrate the chemical behaviour.

CONCLUSIONS

The discretization technique presented makes it possible to calculate mass transfer behaviour of a typical, highly complicated chemical sorption/reaction system, without convergence or stability problems over a wide range of conditions. The difference between the numerically obtained solutions and those of previous workers was less than 1% for those cases where exact analytical solutions were available. As can be expected, the previously published approximate solutions, obtained via linearization techniques, differ somewhat more (up to 7%) but the agreement was still remarkable.

Further, it has been shown that the (approximate) solutions for absorption calculations are also valid for desorption. At simultaneous mass transfer special attention has been paid to the reversibility effects in the mass transfer zone. It has been shown how negative enhancement factors can occur for conditions when the absorption of one of the gases forces the other to desorb by induced reversibility in the liquid transfer zone, though the driving forces would predict that both gases would absorb. This implies that at simultaneous absorption of two gases accompanied by interfering reactions the sign of the driving forces alone does not ensure the direction of mass transfer.

By forced transfer zone conditions desorption might occur. It has been supplementarily demonstrated that at simultaneous absorption and desorption, the absorbing component can also activate, i.e. "over-enhance" and even infinitely overenhance, the desorbing one.

It may be concluded from this contribution that the availability of a stable discretizations technique not only makes it possible accurately to calculate mass transfer behaviour for a very complex reacting system, thus avoiding possible miscalculation by using linearization techniques, but may also reveal new insights into sorption behaviour.

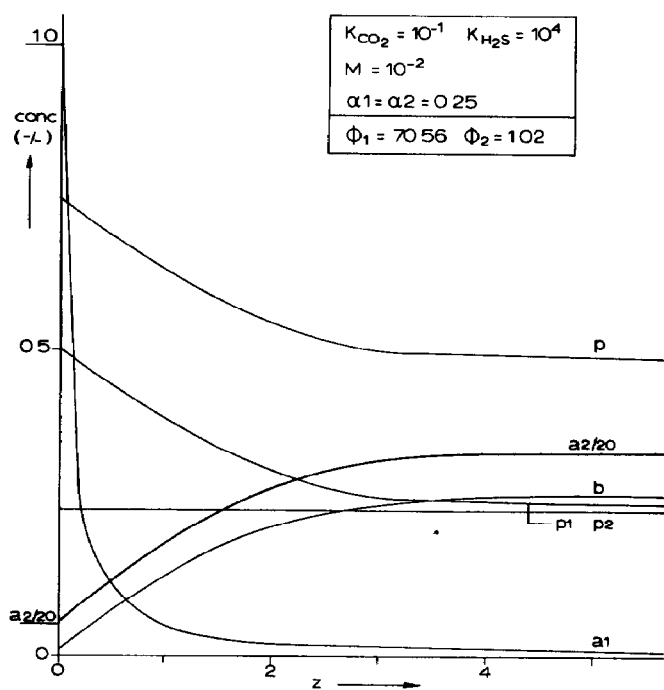


Fig 9

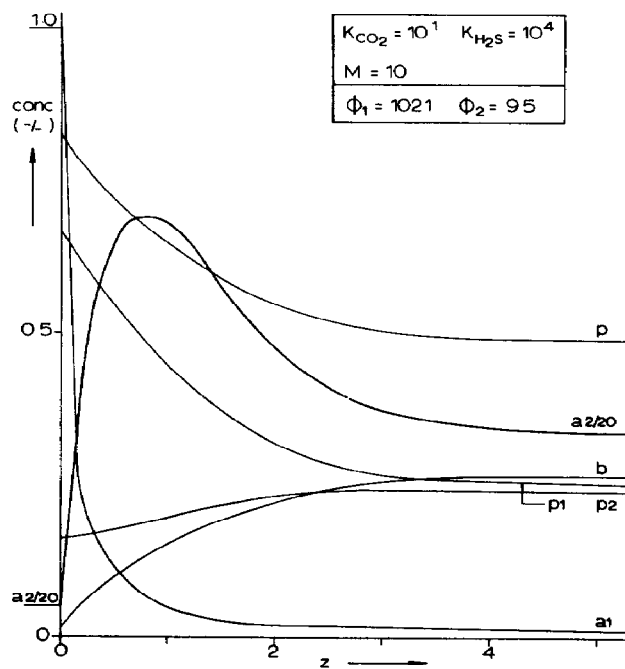


Fig 10

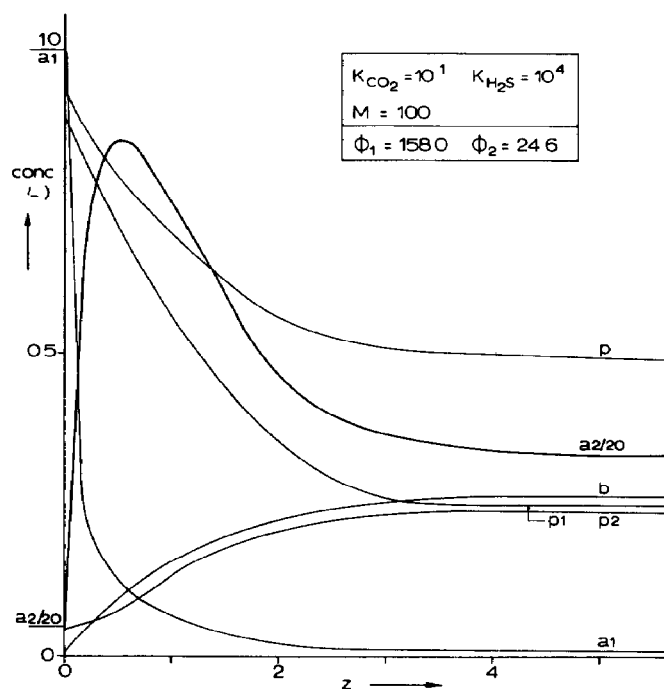


Fig 11

Figs 9–11 Pictures of the numerically calculated dimensionless concentration profiles in the liquid at simultaneous transfer of H_2S (a_1) and CO_2 (a_2) accompanied by reactions. Figure 9 shows the profiles for one particular condition of Figure 8 ($M = 10^{-2}$) for curve 5. Figures 10 and 11 show the effect of an increase in M on the profiles and enhancement factors.

NOTATION

A	coefficient matrix defined in eqn (23)
a_1, a_2	$[H_2S]/(m_1 [H_2S]_g)$, $[CO_2]/(m_2 [CO_2]_g)$
Am	total amine concentration, see eqn (11)
b	$[R_2NH]/Am$
B	concentration vector defined in eqn (23)
C_1, C_2	total H_2S conc, eqn (9), total CO_2 conc, see eqn (10)
D_i	liquid diffusion coefficient of component i
h	distance step in the liquid
k	time step in penetration period
k_2	reaction rate constant
kg_1, kg_2	mass transfer coefficient of H_2S and CO_2 respectively in gas phase
kl_1, kl_2	idem in the liquid phase ($= 2\sqrt{D_{CO_2}/(\pi\tau)}$ $2\sqrt{D_{H_2S}/(\pi\tau)}$)
K_i	equilibrium constant of reaction species i
K_1, K_2	q_1/K_{H_2S} $q_2/(K_{CO_2} Am)$
p, pl	$[R_2NH_2^+]/Am$, $[HS^-]/Am$
p_2, p_3	$[R_2NCOO^-]/Am$, $[HCO_3^-]/Am$
m_1, m_2	physical equilibrium constant of H_2S and CO_2 respectively defined as conc in the liquid phase over that in the gas phase
M	$\pi k_2 \tau Am/4$
$\mathcal{O}(h, k)$	order symbol quantity roughly proportional with h and k
q_1, q_2	$Am/(m_1 [H_2S]_g)$, $Am/(m_2 [CO_2]_g)$
r	unspecified constant
r_i	D_i/D_{CO_2}
R	net conversion rate per unit volume
t	time variable
U_i^j	concentration vector U evaluated at i distance steps and j time steps
x	distance variable
z	$2x/\sqrt{\pi\tau D_{CO_2}}$

Greek symbols

α, β	unspecified constants
α_1, α_2	C_1/Am , C_2/Am
ϕ_1, ϕ_2	enhancement factors defined by eqns (18) and (19)
τ, θ	contact time according to the Higbie model t/τ
$\xi(z)$	transformation function of distance parameter z
$\omega(\phi)$	transformation function of time parameter θ

Indices

g	gas phase
l	liquid phase
o	at the interface
∞	at infinite depth in the liquid
[]	concentration

REFERENCES

- [1] Goettler L A and Pigford R L, *I Chem E Symp Ser* 1968 28
 [2] Olander O R, *AIChE J* 1960 6 233

- [3] Onda K, Sada E, Kobayashi T and Fujine M, *Chem Engng Sci* 1970 25 761
 [4] Onda K, Sada E, Kobayashi T and Fujine M, *Chem Engng Sci* 1970 25 1023
 [5] Onda K, Sada E, Kobayashi T and Fujine M, *Chem Engng Sci* 1970 25 753
 [6] Onda K, Sada E, Kobayashi T and Fujine M, *Chem Engng Sci* 1971 26 247
 [7] Ouwerkerk C, *I Chem E Symp Ser* 1968 28 39
 [8] Ramachandran P A and Sharma M M, *Chem Engng Sci* 1972 27 1807
 [9] Ramachandran P A and Sharma M M, *Chem Engng Sci* 1971 26 349
 [10] Ramachandran P A and Sharma M M, *Trans Instn Chem Engrs* 1971 49 253
 [11] Shah Y T and Sharma M M, *Trans Instn Chem Engrs* 1976 54 1
 [12] Hikita H and Asai S, *Kagaku Kogaku* 1963 27 823
 [13] Van Krevelen D W and Hofstuzer P J, *Rec Trav Chim* 1948 67 563
 [14] Cornelisse R, Beenackers A A C M and Van Swaay W P M, *Chem Engng Sci* 1977 33 1532
 [15] Goettler L A and Pigford R L, *AIChE J* 1971 17 793
 [16] Danckwerts P V and Sharma M M, *Chem Engng* 1966 10 244
 [17] Ouwerkerk C, Paper presented at *Natural Gas Processing and Utilization Conference*, Dublin 1976
 [18] Ouwerkerk C, *Hydrocarb Proc* 1978 4 89
 [19] Danckwerts P V, *Gas-Liquid Reactions*, McGraw-Hill, New York 1970
 [20] Danckwerts P V and McNeil K M, *Trans Instn Chem Engrs* 1967 45 32
 [21] Astarita G, Gioia F and Balzano C, *Chem Engng Sci* 1965 20 1101
 [22] Gioia F, *Chim Ind* 1967, 49(9) 921
 [23] Tavares da Silva A and Danckwerts P V, *Instn Chem E Symp Ser* 1968 28 48
 [24] Baker G A and Oliphant T A, *Quart Appl Math* 1960 17(4) 361
 [25] Stoer J, *Einführung in die Numerische Mathematik I*, p 192 Springer Verlag, Berlin 1971
 [26] Secor R M and Beuttler J A, *AIChE J* 1967 13 365
 [27] De Coursey W J, *Chem Engng Sci* 1974 29 1867
 [28] Wellek R M, Brunson R J and Law F H, *Can J Chem Engng* 1978 56 181
 [29] Yeramian A A, Gottifredi J C and Ronco J J, *Chem Engng Sci* 1970 25 1622
 [30] Danckwerts P V, *Chem Engng Sci* 1968 23 1045 (A2) (7-5-8)

APPENDIX I

After rearrangement of the original set of eqns (4)-(17) (as indicated between the brackets) a new set of dimensionless differential equations can be denoted (A1)-(A16), which is suitable for numerical treatment

$$\frac{1}{q_1} \frac{\partial a_1}{\partial \theta} + \frac{\partial p_1}{\partial \theta} = \frac{4}{\pi} \left\{ r_{a_1} \frac{\partial^2 a_1}{\partial z^2} + r_{p_1} \frac{\partial^2 p_1}{\partial z^2} \right\} \quad (A1) (6)$$

$$\frac{\partial b}{\partial \theta} - \frac{2}{q_2} \frac{\partial a_2}{\partial \theta} - \frac{1}{q_1} \frac{\partial a_1}{\partial \theta}$$

$$= \frac{4}{\pi} \left\{ r_b \frac{\partial^2 b}{\partial z^2} - \frac{2}{q_2} \frac{\partial^2 a_2}{\partial z^2} - \frac{r_{a_1}}{q_1} \frac{\partial^2 a_1}{\partial z^2} \right\}$$

(A2) (7-5-8)

$$\frac{1}{M} \frac{\partial a_2}{\partial \theta} = \frac{4}{\pi} \frac{1}{M} \frac{\partial^2 a_2}{\partial z^2} - a_2 b + K_2 p_2 p/b \quad (A3) (4)$$

$$\frac{\partial p}{\partial \theta} + \frac{1}{q_1} \frac{\partial a_1}{\partial \theta} + \frac{1}{q_2} \frac{\partial a_2}{\partial \theta} = \frac{4}{\pi} \left\{ r_p \frac{\partial^2 p}{\partial z^2} + \frac{ra_1}{q_1} \frac{\partial^2 a_1}{\partial z^2} + \frac{1}{q_2} \frac{\partial^2 a_2}{\partial z^2} \right\} \quad (\text{A4}) \quad (8)$$

$$\frac{1}{q_2} \frac{\partial a_2}{\partial \theta} + \frac{\partial p_2}{\partial \theta} = \frac{4}{\pi} \left\{ \frac{1}{q^2} \frac{\partial^2 a_2}{\partial z^2} + r_{p2} \frac{\partial^2 p_2}{\partial z^2} \right\} \quad (\text{A5}) \quad (5)$$

$$ba_1/(pp_1) = K_1 \quad (\text{A6}) \quad (1)$$

The boundary conditions at $z = 0$ are

$$1 - a_2 = -m_2 kl_1/kg_2 \left(\frac{\partial a_2}{\partial z} \right) \quad (\text{A7}) \quad (13)$$

$$1 - a_1 = -m_1 kl_2/kg_1 \left(\frac{\partial a_1}{\partial z} \right) \quad (\text{A8}) \quad (14)$$

$$r_b \frac{\partial b}{\partial z} + r_p \frac{\partial p}{\partial z} = 0 \quad (\text{A9}) \quad (15)$$

$$\frac{\partial p_2}{\partial z} = 0 \quad (\text{A10}) \quad (16)$$

$$r_b \frac{\partial b}{\partial z} + r_{p1} \frac{\partial p_1}{\partial z} = 0 \quad (\text{A11}) \quad (17)$$

and at $(\theta = 0, z \neq 0)$ and $(\theta \neq 0, z = \infty)$

$$p_2 + a_2/q_2 = \alpha_2 \quad (\text{A12}) \quad (9)$$

$$p_1 + a_1/q_1 = \alpha_1 \quad (\text{A13}) \quad (10)$$

$$b + p_2 + p = 1 \quad (\text{A14}) \quad (11)$$

$$a_2 b^2/(pp_2) = K_2 \quad (\text{A15}) \quad (2)$$

$$ba_1/(pp_1) = K_1 \quad (\text{A6}) \quad (1)$$

$$p_2 + p_1 + p_3 = P \quad (\text{A16}) \quad (12)$$